

# Existence of a short period (3.5-4 hours) in the photometric variability of WR 66\*

G. Rauw<sup>1, \*\*</sup>, E. Gosset<sup>1, \*\*\*</sup>, J. Manfroid<sup>1, †</sup>, J.-M. Vreux<sup>1</sup>, and J.-F. Claeskens<sup>2</sup>

<sup>1</sup> Institut d’Astrophysique, Université de Liège, 5, avenue de Cointe, B-4000 Liège, Belgium

<sup>2</sup> European Southern Observatory, Casilla 19001, Santiago 19, Chile

Received 7 March 1995 / Accepted 4 July 1995

**Abstract.** We report here on an independent detection of a short period ( $\sim 4$  hours) in the photometric variations of WR 66, thus confirming in broad terms the discovery by Antokhin et al. (1995). In addition, we present the first spectroscopic variability analysis for this star. A few peculiarities of the spectrum of WR 66 are also discussed. Finally, we perform a brief examination of different possible origins of the phenomenon.

**Key words:** stars: individual: WR 66 – stars: Wolf-Rayet – stars: mass-loss – stars: variables

## 1. Introduction

WR 66 ( $\equiv$  HD 134877  $\equiv$  LSS 3322) is a Wolf-Rayet (hereafter WR) star of spectral type WN 8 with a visual magnitude  $v = 11.71$  (van der Hucht et al., 1981) in the *ubvr* photometric system of Westerlund (1966).

Lortet et al. (1987) have discussed the reddening and distances of hot stars in the region of WR 66, and their conclusion is that all the OB and WR stars of this area belong to the same stellar association previously named Cir OB1. This association contains the cluster Pis 20 for which they definitely put forward a distance of about 4 kpc. WR 66 is located at the southern periphery of Cir OB1 but Lortet et al. (1987) point out that this is a common feature of the WN 8 stars in the LMC, which are found isolated or peripheral (a fact also mentioned by Moffat, 1989). Consequently, they suggest to adopt the same distance modulus for WR 66 as for the cluster, i.e.  $DM = m_0 - M = 13.0$ .

Over the years, values of  $E(b-v)$  for WN stars have been determined using various approaches which are comprehensively

compared in Schmutz & Vacca (1991). For WR 66, these authors adopt a value  $E(b-v) = 0.90$ . A more recent determination by Hamann et al. (1993) uses a different technique (more model dependent) to derive  $(b-v)_0$ : this method leads to  $E(b-v) = 1.0$ , i.e. a value very close to the previous ones, considering that Hamann et al. (1993) find their values to be systematically in excess with respect to those of Schmutz & Vacca (1991) by about 0.1. Both approaches are however not completely independent. Then, it is possible to derive  $A_v$  through the relation between  $A_v$  and  $E(b-v)$  given by Lundström & Stenholm (1984) and, finally, to get  $M_v = m_v - DM - A_v = -5.2$ . From this value and using their models, Hamann et al. (1993) derive a value for the mass-loss rate:  $\log |M| = -4.5$ . It is interesting to note that, considering WR stars of similar luminosity, this value means that WR 66 is among the objects with the lowest mass-loss rate (Hamann et al., 1993). This result is less supported by the revised values given by Hamann et al. (1995); one should therefore be cautious. Other interesting characteristics of WR 66 are its low luminosity (for a late WN) and the presence of a small amount of residual hydrogen in its atmosphere, two aspects which are best seen on Fig. 3 of Hamann (1995) and on Fig. 6 of Hamann et al. (1995).

As far as photometric variability is concerned, WR 66 was included in the monitoring of southern WR stars conducted by Lamontagne & Moffat (1987), who conclude that WR 66 varies with a lower amplitude than the other WN 8 stars of their survey, with a possible period of  $P = 4.25$  days (peak-to-peak  $\Delta V = 0.06$  mag,  $\sigma_V = 0.015$  mag). Nevertheless, they caution that the reality of this period is marginal and subject to confirmation. As a matter of fact, Fig. 2 of Moffat & Robert (1991), which refers to a larger sample, clearly shows that WR 66 is the WN 8 star with the lowest photometric variability.

This star was also included in the high speed photometry survey (time resolution  $\Delta t = 0.005$  s) conducted by Marchenko et al. (1994): no very short time-scale (0.01 Hz–100 Hz) periodic variability has been detected.

Finally, WR 66 has been intensively observed, during some three consecutive months in 1993, by Antokhin et al. (1995), with a single-channel photometer equipped with a broadband  $V$

Send offprint requests to: E. Gosset

\* Based on observations collected at the European Southern Observatory, La Silla, Chile.

\*\* Aspirant au Fonds National de la Recherche Scientifique.

\*\*\* Chercheur Qualifié au Fonds National de la Recherche Scientifique.

† Directeur de Recherches au Fonds National de la Recherche Scientifique.

filter. They report a standard deviation of the differential magnitudes of  $\sigma = 0.0151$  for the WR star, to be compared to  $\sigma = 0.0062$  for the comparison stars (HD 134819 and HD 134893) and discover that WR 66 is probably variable with a period of 3.51 hours (i.e. a frequency  $\nu = 6.828 \text{ d}^{-1}$ , and a peak-to-peak amplitude of about  $\Delta V = 0.021 \text{ mag}$ ). However, Antokhin et al. (1995) are very cautious in their conclusions because they suspect the existence of some variability (at low frequency) in the comparison stars they used for WR 66 and, also, because a frequency half the reported one is detected in the comparison stars of WR 82.

Several years ago, we initiated a detailed study and/or re-analysis of WR star variability (see Gosset et al., 1994a). We will present here our own photometric and spectroscopic observations of WR 66. Sect. 2 describes the various instruments and techniques used during our campaigns. In Sect. 3, we show that we independently detected, in our photometric data, a high frequency we further show to be compatible with the results of Antokhin et al. (1995). In Sect. 4, we present our spectroscopic observations: they indicate that sizeable variations are taking place in the mass ejection process of WR 66. Finally, Sect. 5 contains a discussion of the various results.

## 2. Observations

### 2.1. Photometry

The photometric data were acquired at the European Southern Observatory (ESO, La Silla) at the ESO 1m telescope equipped with the standard one-channel photometer. A first run took place in April 1989 (JD2447592–7599) and a second one in June 1989 (JD2447700–7715). The only filter used was ESO nr.324 (Schwarz and Melnick, 1993) which corresponds to a Strömgren *b* filter; the diaphragm was kept at 23''. The observations of April consist of the sequence C<sub>1</sub> V sky C<sub>2</sub>, whereas those of June consist of the sequence V sky C<sub>2</sub> C<sub>1</sub> X<sub>1</sub> X<sub>2</sub>, where V is the variable WR star WR 66, while C<sub>1</sub> and C<sub>2</sub> are the comparison stars: respectively, HD 139915 (G0Ib) and HD 144481 (A3mA7–F2). The X<sub>i</sub> are other program stars studied simultaneously (namely WR 69 and WR 71). These latter objects will not be further studied in the present paper. The sequence is usually repeated four times, the whole tight set taking about 25 to 33 min. Each individual measurement is made of short (5 s) integrations totalling some 40 to 100 s. Several sets of four sequences were performed each night, usually spaced by about 1h30min to 1h45min (sometimes the dispersion around this mean value is quite large, particularly for the June subset). The remainder of the observing time was devoted to other WR stars (see, for example, dataset III on WR 16 in Gosset et al., 1990).

These data have been reduced as a whole using a procedure based on the method outlined by Sterken & Manfroid (1992). The magnitudes of the comparison stars have been interpolated to the time of the observations of the WR star; differential magnitudes of the type V–(C<sub>1</sub>+C<sub>2</sub>)/2 and C<sub>1</sub>–C<sub>2</sub> have been computed. The contemporaneous differential magnitudes of the first type are given in Table 1. The whole set of observations consists

of 135 values (dataset A), distributed as 48 values from April (dataset B) and 87 from June (dataset C). We defined also a fourth dataset containing all the observations but averaged over the tight sets of four sequences; this latter dataset labelled M contains 40 values. The mean values and standard deviations of the different datasets are given in Table 2.

### 2.2. Spectroscopy

Our first spectroscopic observations of WR 66 date back to February 1982, when we acquired two spectra (S/N  $\simeq 70$ –100 in the continuum) in the red region with the ESO Reticon system (Dennefeld et al., 1979) attached to the Boller & Chivens spectrograph at the ESO 1.5m telescope. The slit used was 150  $\mu\text{m}$  wide which corresponds to 3'' on the sky and to about 32  $\mu\text{m}$  ( $\sim 7.6 \text{ \AA}$ ) in the plane of the detector; this is somewhat larger than a diode (25.4  $\mu\text{m}$ ) but comparable to the full width at half maximum of the experimental profile (30–35  $\mu\text{m}$  according to Dennefeld et al., 1979). The domain covered was 5700–10890  $\text{\AA}$ . These observations were performed in the context of a red survey of Southern Galactic WR stars (Vreux et al., 1983).

Blue spectra of WR 66 covering the wavelength domain 3860–4220  $\text{\AA}$  were obtained in May 1986 with the first UV-coated GEC CCD (ESO CCD#6; ESO, 1985) attached to the Boller & Chivens spectrograph at the ESO/MPI 2.2m telescope (S/N  $\simeq 50$  in the continuum). The slit was set to 171  $\mu\text{m}$  (2'' on the sky) which, projected on the detector, corresponds to about 19.2  $\mu\text{m}$  to be compared to the 22  $\mu\text{m}$  pixel size. The first order was blocked via a 2 mm BG 39 filter and the second order reciprocal dispersion was 29  $\text{\AA mm}^{-1}$  corresponding to 0.64  $\text{\AA}$  per pixel. Two 30 min spectra were acquired during the night May 24/25, three 45 min spectra during the night May 25/26 and two on May 27/28.

Later, we decided to acquire time-resolved spectroscopy of WR 66 and a small campaign was organized in 1994. The 1994 spectroscopic data were acquired at the ESO 1.5m telescope equipped with a Boller & Chivens Cassegrain spectrograph. The detector used was a Ford Aerospace 2048L UV-coated CCD (ESO CCD#24, Schwarz & Melnick, 1993) with a square pixel size of 15  $\mu\text{m}$  corresponding to 0''.81 on the sky in the spatial direction. The conversion factor was 2.9 e<sup>–</sup>/ADU. A first two-night run took place on April, 28/30 1994; grating ESO#32, which was used, is a holographic grating with 2400 lines/mm giving a reciprocal dispersion of 32.6  $\text{\AA mm}^{-1}$  ( $\sim 0.5 \text{ \AA}$  per pixel). The domain covered was 3875–4875  $\text{\AA}$ . The seeing was very good for the first night ( $\lesssim 1''$ ) but it got worse during the second one ( $> 1''.5$ ). It appeared that the grating used on these nights was suffering from astigmatism due to a loose mounting. The second run consists of only one night of observations of WR 66, namely May, 21/22 1994. In this latter case, the grating was a conventional one (ESO#22), with 1200 lines/mm and giving a second order reciprocal dispersion of 32.8  $\text{\AA mm}^{-1}$ . The domain covered was 3905–4893  $\text{\AA}$ . Bad seeing and strong wind prevailed during this last night.

**Table 1.** Differential Strömgren  $b$  magnitudes for WR 66 as a function of the heliocentric Julian date

JD 2440000+	$\Delta b$						
7592.76261	4.8990	7597.72844	4.8986	7704.64754	4.9047	7711.52688	4.9150
7592.76764	4.8972	7597.73318	4.8959	7704.65394	4.9021	7711.59354	4.9081
7592.77272	4.8946	7597.80816	4.9141	7704.66003	4.9053	7711.59992	4.8992
7592.77742	4.9061	7597.81289	4.9191	7704.66722	4.9030	7711.60863	4.9013
7592.86080	4.9235	7597.81766	4.9141	7704.75099	4.8955	7711.61525	4.9085
7592.86545	4.9173	7597.82198	4.9168	7704.75831	4.8944	7711.71233	4.9008
7592.87094	4.9246	7598.71195	4.9068	7704.76522	4.8975	7711.71890	4.9000
7592.87536	4.9265	7598.71642	4.9097	7704.77205	4.9008	7711.72522	4.8942
7593.76681	4.9061	7598.72065	4.9072	7705.54910	4.9072	7711.73156	4.8998
7593.77119	4.8927	7598.72510	4.9070	7705.55549	4.9151	7712.48812	4.9064
7593.77797	4.9033	7598.80304	4.8869	7706.47696	4.9094	7712.49416	4.9136
7593.78234	4.8985	7598.80768	4.8919	7706.48375	4.9081	7712.50116	4.9078
7595.75867	4.9130	7598.81210	4.8900	7706.52102	4.9240	7712.50749	4.9167
7595.76388	4.9141	7598.82101	4.9025	7706.52722	4.9201	7712.56644	4.9211
7595.76906	4.9134			7706.60267	4.9040	7712.57257	4.9153
7595.77551	4.9158	7700.59557	4.9124	7706.60938	4.9104	7712.57969	4.9231
7595.84702	4.9143	7700.61212	4.9080	7706.65339	4.9103	7712.58645	4.9143
7595.85106	4.9168	7700.62223	4.9110	7706.65945	4.9106	7712.70122	4.9290
7595.85586	4.9125	7700.63695	4.9015	7706.70967	4.9266	7712.70874	4.9287
7595.86056	4.9068	7700.77501	4.9145	7706.71596	4.9146	7712.71517	4.9265
7596.72010	4.8942	7700.78196	4.9002	7706.76549	4.9066	7712.72172	4.9321
7596.72516	4.8949	7700.78886	4.9114	7706.77180	4.9054	7714.51998	4.8980
7596.72934	4.8946	7700.79641	4.9225	7706.79679	4.9050	7714.52627	4.9090
7596.73353	4.8833	7701.49295	4.9230	7706.80330	4.9054	7714.53280	4.9129
7596.79654	4.9052	7701.50151	4.9274	7707.48317	4.9100	7714.53810	4.9140
7596.80134	4.9039	7701.50879	4.9307	7707.48981	4.9026	7714.54448	4.9093
7596.80590	4.9087	7702.51171	4.9214	7707.49634	4.9067	7714.60318	4.9205
7596.81039	4.9135	7702.51941	4.8995	7707.50301	4.8937	7714.61013	4.9204
7596.86116	4.8987	7702.52660	4.9093	7707.60004	4.9168	7714.61548	4.9282
7596.86610	4.9016	7702.53507	4.9170	7707.60700	4.9148	7714.62154	4.9183
7596.87014	4.8935	7702.59607	4.9143	7707.65146	4.9042	7714.70473	4.9043
7596.87396	4.8936	7702.60390	4.9087	7711.50676	4.9146	7714.71146	4.9078
7597.71917	4.9021	7702.61171	4.9131	7711.51442	4.9173	7714.71836	4.9150
7597.72415	4.8984	7702.61870	4.9123	7711.52067	4.9216	7714.72426	4.9218

**Table 2.** Mean and standard deviation of the differential Strömgren  $b$  magnitudes relative to the different datasets

Dataset	V–(C <sub>1</sub> +C <sub>2</sub> )/2		C <sub>1</sub> –C <sub>2</sub>	
	$\bar{\Delta b}$	$\sigma_{\Delta b}$	$\bar{\Delta b}$	$\sigma_{\Delta b}$
A	4.9091	0.0100	0.4978	0.0045
B	4.9051	0.0102	0.4969	0.0032
C	4.9113	0.0092	0.4983	0.0050
M	4.9096	0.0091	0.4976	0.0042

During the three nights, 47 spectra of WR 66 (respectively, 14, 20 and 13) were recorded. Exposure times were typically 20 to 30 min with roughly 20 to 45 min between exposures. A S/N ratio of 30–40 (per pixel) characterizes all the spectra.

All the reductions were performed using standard procedures in the IHAP application package and in a cautiously checked version of the MIDAS one, both developed at ESO.

The wavelength scale was derived through comparison with HeAr spectra acquired with the telescope in the same positions as for the science exposures. Dome flat-fields were utilized. The response curve was derived from observations of the spectrophotometric standard stars LTT 3218, LTT 4364 and EG 274. The reduced spectra were normalized to the continuum by using a polynomial fit through carefully chosen continuum windows.

### 3. Analysis of the photometric data

#### 3.1. The entire set of photometric data (dataset A)

We analysed the data of dataset A using Fourier techniques specially designed for unevenly sampled data (Deeming, 1975; Scargle, 1982). Some of the results are displayed in Fig. 1 for frequencies up to  $12.5 \text{ d}^{-1}$ , thus displaying the whole zone of interest. The power spectral window (Fig. 1a) exhibits, besides the zero frequency peak, one-day aliasing as evidenced by the presence of a peak at  $\nu = 1.002 \text{ d}^{-1}$  (75 % in power) and another

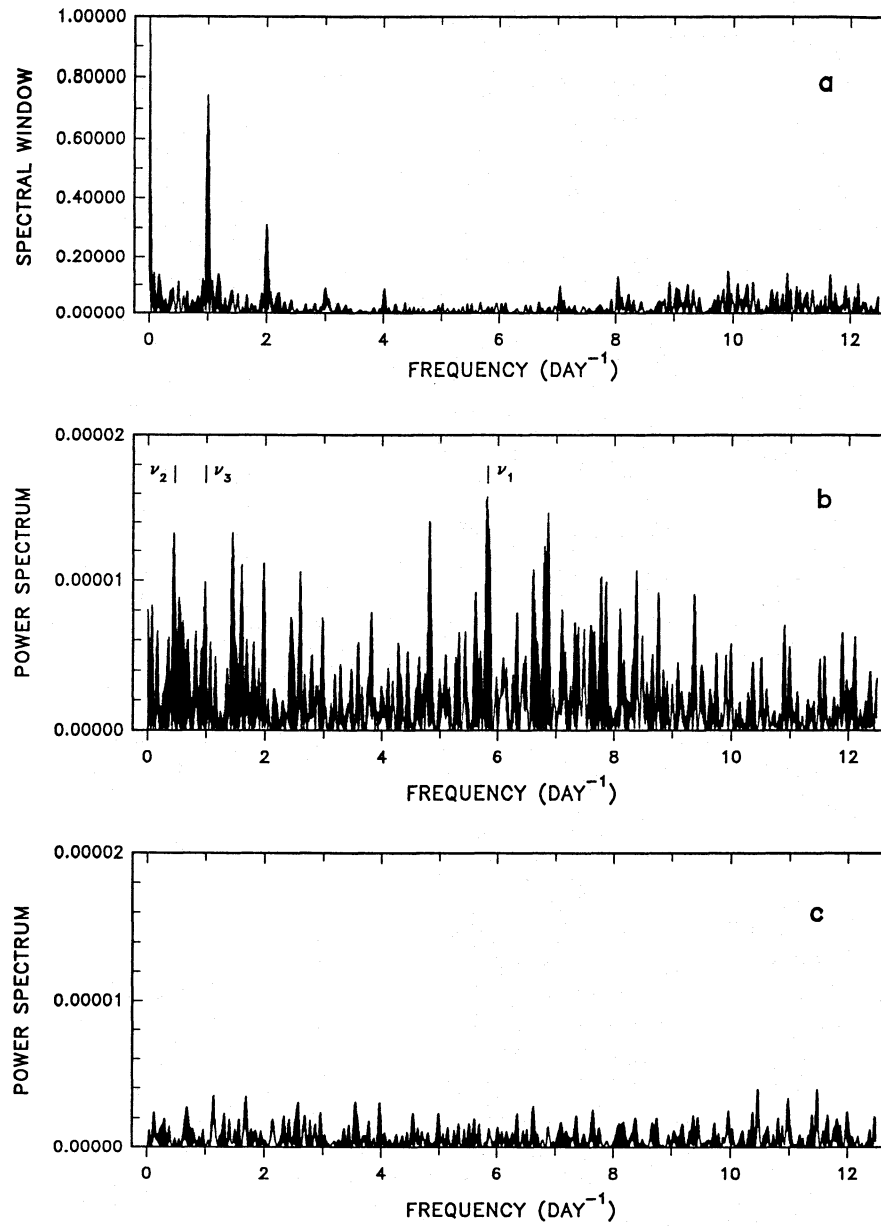


**Fig. 1a–c.** Power spectrum analysis of the differential magnitudes of Table 1 using the method of Deeming (1975): **a** the power spectral window, **b** the power spectrum of the differential magnitudes, **c** the power spectrum of the differential magnitudes prewhitened for  $\nu_1 = 5.815 \text{ d}^{-1}$ ,  $\nu_2 = 0.444 \text{ d}^{-1}$  and  $\nu_3 = 0.997 \text{ d}^{-1}$ . The abscissae represent the frequency expressed in  $\text{d}^{-1}$ , the ordinate units for part **b** and **c** are square magnitudes

at  $\nu = 2.004 \text{ d}^{-1}$  (30 %). Beyond this, the spectral window is almost empty. These peaks are subdivided in a series of aliases corresponding to the gap between the April and the June runs ( $\Delta\nu \sim 0.009 \text{ d}^{-1}$ ). The power spectrum of the data (Fig. 1b) exhibits the strongest peak at  $\nu_1 = 5.815 \text{ d}^{-1}$  (along with April–June aliases at  $\nu = 5.832 \text{ d}^{-1}$ ,  $5.824 \text{ d}^{-1}$ ,  $5.806 \text{ d}^{-1}$  and many fainter ones) with one-day aliases at  $\nu \sim 6.859 \text{ d}^{-1}$  ( $\nu_1 + 1$ ) and  $\nu \sim 4.813 \text{ d}^{-1}$  ( $\nu_1 - 1$ ). Although it is reasonable to take the highest peak as the progenitor, it should be kept in mind that the choice among the aliases in a power spectrum is always to some extent arbitrary. In particular, the highest peak could correspond to the frequency that gives a lightcurve whose characteristics are the most reminiscent of a sine wave. This is interesting for prewhitening the data, but the frequency having the most physical meaning will not necessarily be favoured; this turns the identification of the true progenitor into a difficult

or even impossible task. In particular, the April–June aliasing visible in the spectral window renders any choice for a true progenitor quite illusory. On the other hand, the one-day aliasing vanishes rapidly and  $\nu_1$  has no outstanding remote alias, particularly in the low frequency ( $\nu_1 < 1 \text{ d}^{-1}$ ) domain, and we can be confident that the phenomenon associated to  $\nu_1$  is indeed a high frequency one.

The second highest peak is situated at  $\nu_2 = 0.444 \text{ d}^{-1}$  with an equally strong alias at  $\nu_2 + 1$  (more precisely at  $\nu = 1.445 \text{ d}^{-1}$ ). We have prewhitened (in the sense used by Gosset et al., 1990) the data for the  $\nu_1$  frequency. This means that we have subtracted from the data a sine-wave whose amplitude and phase have been fitted by a least-squares method. The peak at  $\nu_2$  dominates in the power spectrum of the new dataset; its alias  $\nu_2 + 1$  is now markedly fainter. Other peaks are visible around  $\nu = 0.566 \text{ d}^{-1}$  ( $1 - \nu_2$ ),  $\nu = 0.159 \text{ d}^{-1}$ ,  $\nu = 1.972 \text{ d}^{-1}$  and a

series of peaks around  $\nu = 10.988 \text{ d}^{-1}$ . We have also simultaneously prewhitened the original data for the frequencies  $\nu_1$  and  $\nu_2$ ; the power spectrum of the resultant dataset is dominated by  $\nu = 0.005 \text{ d}^{-1}$  and by its aliases at  $\nu = 0.997 \text{ d}^{-1}$  and at  $\nu = 1.981 \text{ d}^{-1}$ . It is interesting to note that, in the power spectrum of the original data first prewhitened for  $\nu_2$ , the dominating frequency, besides  $\nu_1$  and its aliases, is  $\nu = 0.988 \text{ d}^{-1}$ . We have finally prewhitened the original data for the frequencies  $\nu_1$ ,  $\nu_2$  and  $\nu_3$ , where  $\nu_3 = 0.997 \text{ d}^{-1}$  is the alias yielding the most efficient prewhitening. The original data prewhitened for the above quoted three frequencies have again been Fourier analysed. The resulting power spectrum is given in Fig. 1c; the remaining variance corresponds to  $\sigma = 0.0063$ , a value still somewhat larger than the standard deviations related to the comparison stars (see Table 2). The difference can partly be explained by the comparative faintness of WR 66. Clearly, no further frequency is outstanding and we can consider that the data can be decomposed into the three frequencies  $\nu_1$ ,  $\nu_2$  and  $\nu_3$ , plus possible white-noise variations. A similar result is obtained through the analysis of dataset M: this means that the conclusions are independent of the very high frequency behaviour of the WR. It should however be clear that this decomposition does not necessarily have a physical meaning, but that it is a first step towards the analysis of the data. In addition, the three frequencies are not necessarily true deterministic frequencies, but could correspond to particular realizations of a stochastic process. At this point, we can cast some doubts on the existence of  $\nu_3$ , whose alias at lower frequency  $\nu = 0.005 \text{ d}^{-1}$  corresponds to a time-scale of the order of the span of time of the present data. The present observations are not suited to a reliable analysis of such a frequency; therefore, this frequency will not be further investigated here. Although not completely inadequate, the present observations are not ideal either at making a detailed study of  $\nu_2 = 0.444 \text{ d}^{-1}$ . In this particular case, we need to organize a systematic monitoring of the star as we did for some of the brighter WNL stars (see the kind of work expounded in Gosset et al., 1994a). The strong conclusion of the present analysis is the marked presence of the high frequency  $\nu_1$  around  $\nu \sim 5.8 \text{ d}^{-1}$ . A least-squares fit of a sine-wave of frequency  $\nu_1 = 5.815 \text{ d}^{-1}$  to the data gives a semi-amplitude  $a = 0^m 0075$ .

In order to further ascertain our results, we decided to use other methods than Fourier techniques. One of the large alternative families is the one based on trial periods along with studies of the dispersion of the data in the corresponding phase diagram through variance estimation in different bins. We will particularly retain the statistically sound method named “analysis of variance” (AoV) by Schwarzenberg-Czerny (1989). The three-bin version of the statistic  $\Theta_{\text{AoV}}$  introduced by Schwarzenberg-Czerny (1989) is plotted in Fig. 2 as a function of the trial frequency for dataset A. The statistic plotted in Fig. 2 reacts at three aliased frequencies; the strongest reaction occurs exactly at  $\nu = 5.815 \text{ d}^{-1}$ , which also corresponds to the central alias. This is precisely the frequency  $\nu_1$  detected by the Fourier analysis. For a larger number of bins, the highest subpeak tends to be around  $\nu = 5.808 \text{ d}^{-1}$  but the general position of the global peak always remains unchanged. The same method applied to

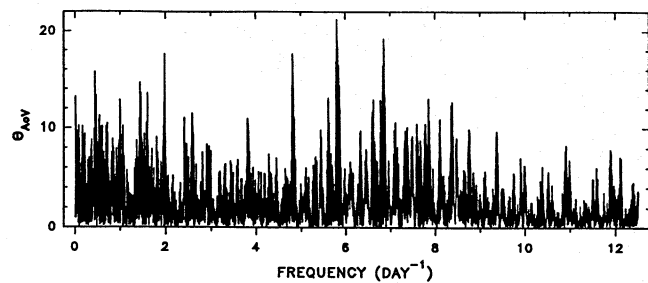


Fig. 2. Plot of the three-bin version of the  $\Theta_{\text{AoV}}$  statistic introduced by Schwarzenberg-Czerny (1989), as a function of the frequency expressed in  $\text{d}^{-1}$  for the differential magnitudes of Table 1. The ordinate units are arbitrary

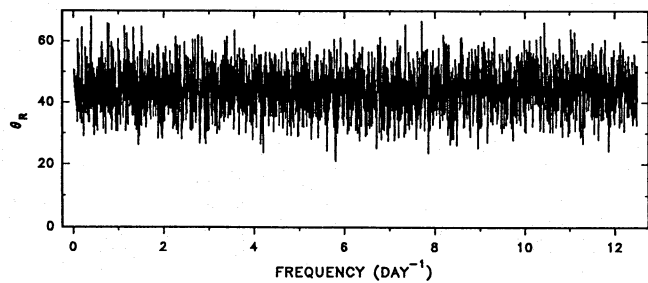


Fig. 3. Plot of the  $\theta_R$  statistic as introduced by Renson (1978), as a function of the frequency expressed in  $\text{d}^{-1}$  for the differential magnitudes of dataset M. The ordinate units are arbitrary

dataset M rather suggests  $\nu = 5.805 \text{ d}^{-1}$ . For some values of the number of bins,  $\nu_2$  and/or its aliases are slightly visible.

We also investigated the data with a trial period string length method; we chose the method described by Renson (1978). The  $\theta_R$  statistic is plotted as a function of the trial frequency for dataset M in Fig. 3. The analysis of dataset A leads basically to the same result, but the disparity of the sampling time-scales makes, as usual, the periodogram more difficult to interpret in the case of a trial period string length method. The dominant deviation in Fig. 3 (here necessarily a minimum) takes place around  $\nu_1$ , definitely confirming the Fourier analysis. The exact position of the deepest minimum is presently at  $\nu = 5.805 \text{ d}^{-1}$ .

We also studied the differential magnitudes  $C_1-C_2$ . The dispersion is evidently less than for WR 66 (see Table 2). The power spectrum of all the differential magnitudes of the comparison stars contains two families of peaks: the first one is at  $\nu = 0.092 \text{ d}^{-1}$ , whereas the second one is at  $\nu = 0.320 \text{ d}^{-1}$  (they are present with their  $1 - \nu$  and  $1 + \nu$  aliases). Outside these values, the spectrum is rather empty; this is particularly true around  $\nu_1$  and  $\nu_2$ .

### 3.2. The partial datasets B and C

We also analysed the two runs of observations separately. The Fourier analysis of the data from the April run (dataset B) leads to a strongly dominant frequency at  $\nu = 5.83 \text{ d}^{-1}$  and to its equally valid one-day aliases (particularly  $\nu - 1$ ). The natural width of the different peaks is of course larger and the quoted

frequency should not be considered as precise. Indeed, this frequency is perfectly compatible with  $\nu_1$ . A second family of aliases with  $\nu = 1.42 \text{ d}^{-1}$  is also present and is most probably related to  $\nu_2$ . Finally, a third family with  $\nu = 7.66 \text{ d}^{-1}$  as the main peak is also visible, but it can be related through aliasing to either  $\nu_1$  or  $\nu_2$ , as evidenced by the analysis of the relevant prewhitened data.

The power spectrum of dataset C presents for its part  $\nu = 1.441 \text{ d}^{-1}$  as its highest peak. The one-day aliasing is not very strong, but it is sufficient for  $\Delta\nu \sim \pm 1 \text{ d}^{-1}$  to associate this frequency with  $\nu_2$ . A second family appears at  $\nu = 7.483 \text{ d}^{-1}$  with a one-day alias at  $\nu = 8.482 \text{ d}^{-1}$ . Finally, a third family is also visible with the highest peak around  $\nu = 6.862 \text{ d}^{-1}$ , which is related to  $\nu_1$ . The power spectrum of the dataset C prewhitened for  $\nu = 1.441 \text{ d}^{-1}$  is dominated by the third family, whose highest peak is now at  $\nu = 5.831 \text{ d}^{-1}$ , which is directly identifiable with  $\nu_1$ , and by the new frequency  $\nu = 1.697 \text{ d}^{-1}$ . The second family is strongly weakened, suggesting some link with  $\nu_2$ . Therefore, we conclude that the frequency  $\nu_1$  detected in the whole dataset (dataset A, see Sect. 3.1) is present during both the April and the June observing runs. This also seems to be the case for  $\nu_2$ .

### 3.3. The data of Antokhin et al. (1995)

Recently, Antokhin et al. (1995) investigated the variability of four southern WN8 stars on the basis of intensive photometry. Among these stars, WR 66 was the only one to exhibit rapid variations with a dominant frequency  $\nu'_1 = 6.828 \text{ d}^{-1}$  and a peak-to-peak amplitude of the least-squares sine-wave of  $0^m021$ . The data consisted of 219 observations acquired through a standard broadband  $V$  filter and distributed over 61 nights, covering a total span of 83 days. Decomposition in frequencies of their data by Antokhin et al. (1995) led to  $\nu'_1 = 6.828 \text{ d}^{-1}$ ,  $\nu'_2 = 0.180 \text{ d}^{-1}$ ,  $\nu'_3 = 0.049 \text{ d}^{-1}$ , and  $\nu'_4 = 0.269 \text{ d}^{-1}$ .

We reanalysed the Antokhin et al.'s (1995) data with Fourier as well as other techniques and, as far as  $\nu'_1$  is concerned, we completely confirm their results. However, it should be underlined that these data are characterized by a rather strong one-day aliasing and, although  $\nu'_1 = 6.828 \text{ d}^{-1}$  is almost always associated with the largest deviation, the choice of the true progenitor is therefore still less straightforward than usual, owing to the strength of the one-day aliasing. It should also be mentioned that far away one-day aliases of  $\nu'_1$  are visible in the low frequency domain, although the probability that the progenitor would be there remains very low. On the other hand, the daily coverage of these observations over such a time span gives strong support to the last digits of the value of  $\nu'_1$  as derived by Antokhin et al. (1995). Indeed, the natural width of the peak is about  $0.012 \text{ d}^{-1}$  and the expected precision can be estimated to be at the level of only a few  $0.001 \text{ d}^{-1}$ .

### 3.4. Discussion

Our photometric data point to the existence of a high frequency in the variability of the WR star WR 66. The significance level is

hard to determine. Indeed, the methods of Scargle (1982) and of Schwarzenberg-Czerny (1989) are potentially statistically correct if the evaluation of the significance level is made at a predetermined frequency. On the other hand, the simple statistical behaviour is lost if one looks at the largest deviation among several frequencies; the solution proposed by Scargle (1982) is simply to neglect the leakage phenomenon: this is usually not completely justified. Horne & Baliunas (1986) proposed a correction to the method of Scargle (1982), but, because they mixed several concepts, their correction is basically erroneous. The proof is that, in the very simple case of even sampling, their simulations give an effective number of degrees of freedom that is twice the correct analytical value of half the number of data points. In fact, they confused the effects due to the leakage and those due to the oversampling of the power spectrum. In addition, in the present case, the tested frequency is far beyond the frequency associated with the one-day sampling, which still further complicates the statistical behaviour. In such a case, although we are currently investigating these problems, we prefer not to discuss the significance level associated with  $\nu_1$ . All in all, however, the mere fact that a high frequency is independently found in our data and in those of Antokhin et al. (1995) is a sufficiently convincing argument in favour of its existence.

Of course, we have no proof towards the uniqueness or the stability of this frequency. However, if one assumes that we have a stable frequency, both our data and those of Antokhin et al. (1995) are quite compatible. In fact,  $\nu = 5.815 \text{ d}^{-1}$  (this work) is completely linked to  $\nu = 6.828 \text{ d}^{-1}$  (Antokhin et al., 1995) through aliasing. Under the hypothesis of stability for this high frequency, it is not unreasonable to think that our data induce a better discrimination among the one-day aliases ( $\nu = 5.8 \text{ d}^{-1}$  instead of  $\nu = 6.8 \text{ d}^{-1}$ ), whereas the data of Antokhin et al. (1995) are sufficiently extensive to support the fractional part of the frequency. Therefore, we propose the value  $\nu = 5.828 \text{ d}^{-1}$  ( $P = 4h7min = 0.172 \text{ d}$ ) for the high frequency present in WR 66, although further data are needed to investigate its stability and nature. Both the standard deviation of our WR differential magnitudes and the deduced amplitude of  $\nu_1$  are about two thirds of those reported by Antokhin et al. (1995), who were observing with a broadband  $V$  filter. This is most probably due to differential variability in the continuum and in the lines (see e.g. Gosset et al., 1994a). In fact, one third of the light corresponding to the observation of WR 66 through the Strömgren  $b$  filter originates from the N III  $\lambda\lambda 4634$ –4641 and He II  $\lambda 4686$  lines.

## 4. Analysis of the spectroscopic data

### 4.1. The spectrum of WR 66

Our first observations of WR 66 date back to February 1982. The resulting useful red part of the WR 66 spectrum is shown in Fig. 4 along with some identifications of the detected lines. The most interesting feature on this spectrum is the strong intensity of the N IV  $\lambda\lambda 7103$ –7128 multiplet, which has the largest equivalent width (hereafter EW) reported for a WN 8 star. This

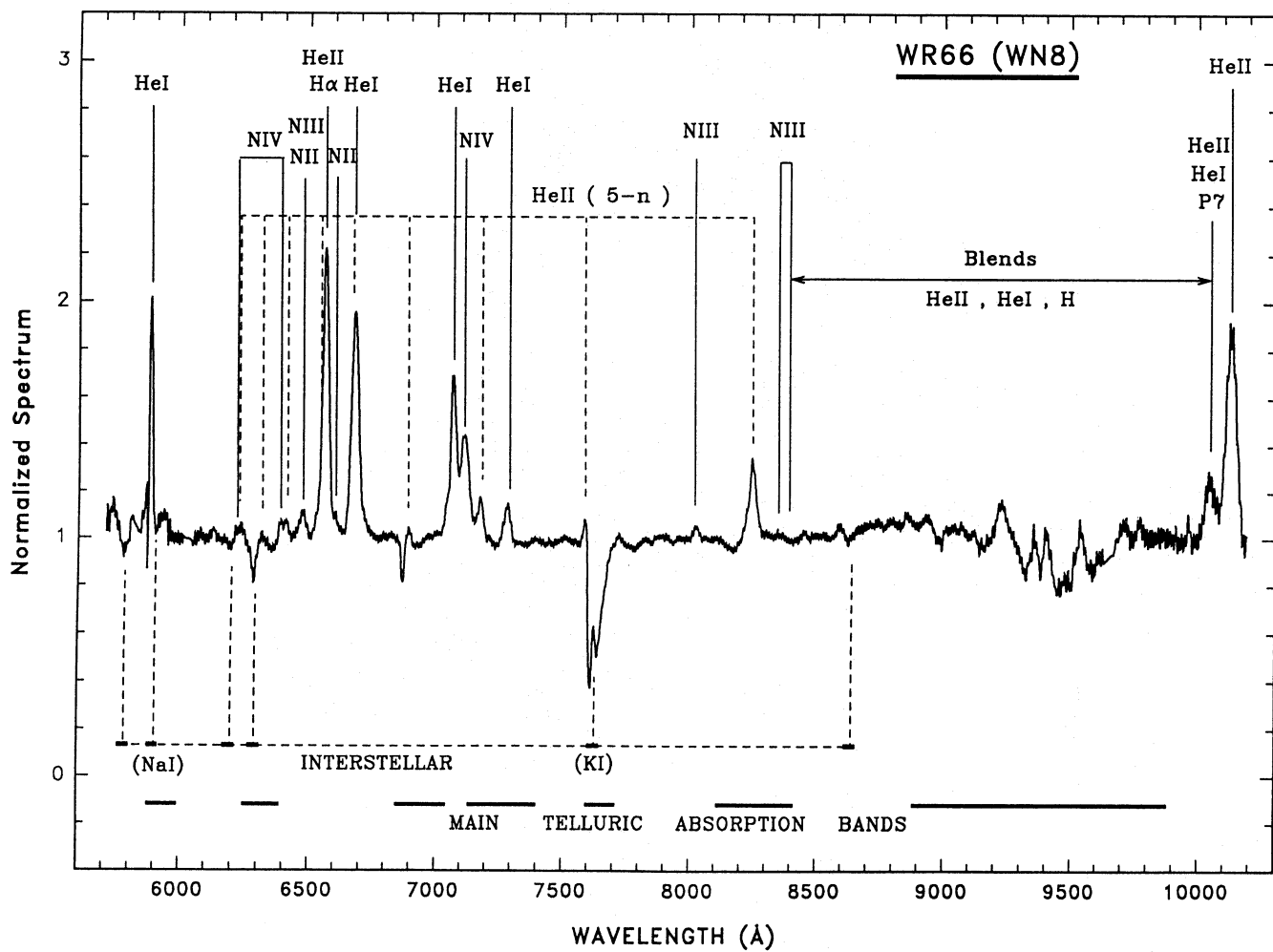


**Fig. 4.** The 1982 spectrum of WR 66, in the red and near infrared domain, as normalized to the continuum. The main lines are identified, above the spectrum for the emissions and below for the absorptions. Interstellar lines and telluric bands are also indicated

can be expressed quantitatively using the Table 1 of Conti et al. (1990) where the EWs are given for eight WN 8 stars. Excluding WR 66, the average EW of N IV  $\lambda\lambda 7103-7128$  for the seven other WN 8 amounts to 8.9 Å, while the value observed for WR 66 is larger than 20 Å. This is less than the intensity observed in a typical WN 7 spectrum, but definitely remarkable for a WN 8 star. Less spectacular, but also indicative, is the intensity of He II  $\lambda 10124$ . In WR 66, its EW is of the order of 63 Å, while the average value observed in five other WN 8 stars is equal to 25.6 Å. This average value is an upper limit as, on the spectra of two other WN 8 stars, He II  $\lambda 10124$  is indeed present but hardly measurable. As far as the He I lines are concerned, they are well developed, as usual in a WN 8 spectrum. Their EWs are comparable to those observed in other WN 8 stars. According to the same reference as above, the average EW of He I  $\lambda 6678$  is equal to 34.5 Å and the one of He I  $\lambda 7065$  equal to 26.3 Å. These average values compare nicely to the values observed in WR 66, i.e. respectively 36 Å and 23 Å.

Other spectra of WR 66, covering the blue domain, were acquired in 1986. To allow a comparison with other late WN

stars, additional objects were observed in 1986 and in 1987 with the same instrumentation: namely two WN 8 stars (WR 16 and WR 40) and four WN 7 stars (WR 12, WR 22, WR 55 and WR 78). Although rather noisy, the blue spectra of WR 66 confirm the peculiar characteristics of the N IV emissions. This can be shown through a comparison, among various objects, of the ratio of the EW of N IV  $\lambda 4058$  to the EW of N III  $\lambda\lambda 3934-3939$ . In the two other WN 8 stars of our sample, this ratio is less than unity, while for the four WN 7 stars, it is of the order of 7. For WR 66, we get an intermediate value, of the order of 2.5, i.e. a ratio markedly larger than for the other WN 8 stars. By itself, this point could just be an academic discussion about an intermediate case in a classification scheme. In WR 66, however, the N IV line is also anomalous in two other ways. First of all, its width is much larger than those observed in the two other WN 8 stars of our sample (FWHM  $\sim 17$  Å compared to 3.6 Å and 5.6 Å for WR 16 and WR 40 respectively). Secondly, and definitely more interesting, the shape of this line is anomalous in the sense that it is less peaked than in the other late WN stars of our sample, i.e. both the WN 8 and the WN 7. To quantify this

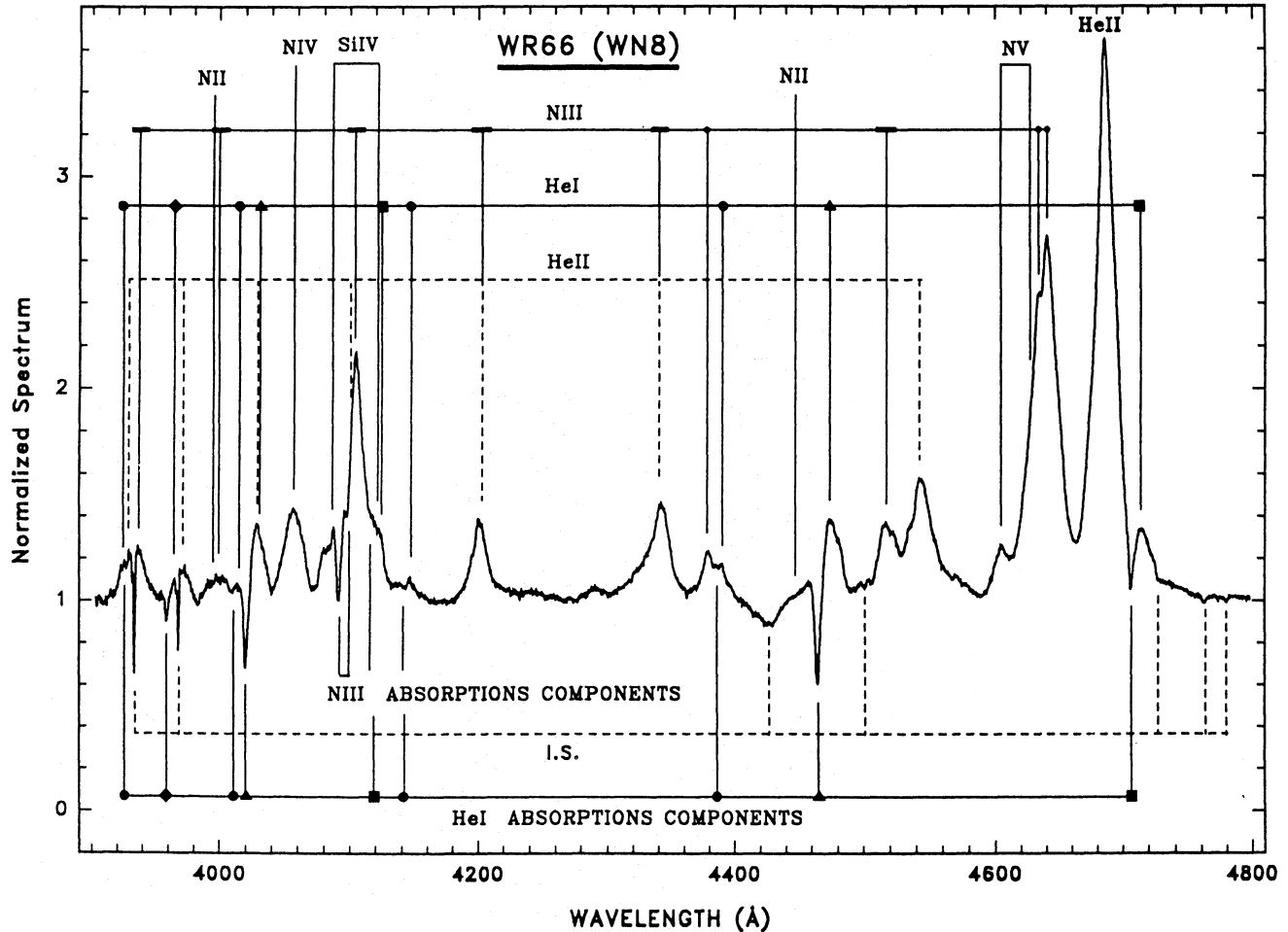


**Fig. 5.** The mean 1994 spectrum of WR 66, in the blue domain, as normalized to the continuum. The main lines are identified, above the spectrum for the emissions and below for the absorptions. For He I, the different systems are marked by filled symbols:  $2^1S - 4^1P^0$  (diamond),  $2^3P^0 - n^3S$  (square),  $2^3P^0 - n^3D$  (triangle) and  $2^1P^0 - n^1D$  (circle). Interstellar lines are also indicated

aspect, we can define a parameter,  $p$ , which is the ratio between the peak intensity (after normalization to the continuum) and the FWHM. In fact, to avoid unnecessary decimals, the ratio  $p = 100\text{\AA} \times I_{\text{max}}/\text{FWHM}$  has been defined and evaluated. For the two WN 8 stars of our sample, this ratio is of the order of  $p = 10$ , and it is larger for WN 7 stars (between 14 and 23). For WR 66, it is less than 3, i.e. remarkably low. This peculiarity of the N IV  $\lambda 4058$  profile in WR 66 can be shown in another way, namely by the comparison between its FWHM and that of He II  $\lambda 4200$ . In all the WN stars of our sample, the FWHM of the He II line is larger than that of the N IV line, whereas the reverse applies to WR 66. Even if it is slightly more difficult to measure, the same is also true for the full width of the line as can be seen on the spectrum displayed on Fig. 5 (more details on this spectrum will be given below). All this means that, in the case of WR 66, the N IV emission region is much more extended than in a typical WN 8-WN 7 star. In WR 66, N IV  $\lambda 4058$  is emitted in a much larger radial velocity domain, in regions much further out in the wind than in any common late WN star. The effect could be global but an alternative view can be found in the relaxation of the spherical symmetry hypothesis. The adoption of

a preferred axis (see e.g. Cassinelli et al., 1995) could turn this anomaly into an orientation effect. Polarimetric studies are, in this respect, a necessary next step. In addition to these particular characteristics of the N IV profile, the 1986 spectra provided another interesting piece of information. As in any classical WN 8, the He I lines are well developed in the spectrum of WR 66, with characteristic P Cygni profiles. Although rather noisy, the 1986 spectra were of sufficient quality to suggest that variations were taking place in the absorption components of the He I P Cygni profiles. The photometric observations described in Sect. 3, for their part, were indicating that a short time-scale was certainly present. Under these circumstances, time resolved spectroscopy was requiring the use of a large telescope. As such an access turned out to be illusory, intensive observations were finally attempted in 1994 with the ESO 1.5m telescope. Though rather noisy, as expected, these observations lead to new interesting pieces of information.

Thus, we acquired some 47 spectra of twenty to thirty minute exposure: the mean of all these 1994 spectra is displayed in Fig. 5 along with the identification of the main lines. The emission lines are due to nitrogen in various stages of ionization

(from N II to N V), to Si IV, to He I and He II. The potential influence of H I lines on the apparent intensities of the He II lines (alternately, along the Pickering  $n$ -4 series) is not easily visible; this is in good agreement with the low H I content reported by Hamann (1995) and Hamann et al. (1995). This small contribution of H I has not been indicated in the figure. As usual in a WN 8 spectrum, the lines of He I are well developed, with a characteristic P Cygni profile. Representative lines of several series are present:  $2^1S - 4^1P^0$ ,  $2^3P^0 - n^3S$ ,  $2^3P^0 - n^3D$ ,  $2^1P^0 - n^1D$  and, on the 1986 spectra, which extend further to the blue,  $2^3S - 3^3P^0$ . Several absorption lines are visible on the figure: they are due to the absorption component of the P Cygni profiles of He I and N III in addition to the usual interstellar absorptions.

#### 4.2. The overall spectroscopic variability of WR 66

The spectroscopic variability of WR 66 has been investigated in several ways. Using a procedure developed for the study of the variability of WR 134, each individual spectrum has been divided by the mean spectrum, giving a series of *mean-normalized spectra* (for more details, see Vreux et al., 1992, and also Gosset et al., 1994b). Let us just recall that, on these mean-normalized spectra, a value different from 1 indicates a temporary deviation from the mean, the deviation being expressed as a percentage of the local intensity. A pixel by pixel variance (over time or spectrum numbering) analysis of these data exhibits well-marked narrow peaks essentially corresponding to the positions of the He I and N III absorptions. Some variations are also detected around the He II  $\lambda 4686$  emission, but the relevant peak in the variance diagram is markedly lower and larger ( $\gg 10 \text{ \AA}$ ). We will come back to this point in the next section. Nevertheless, it is important to remember that the analysed data are rather noisy and that only the strongest variations can be detected. A cross-correlation analysis of the deformation pattern appearing on a given line (see again Vreux et al., 1992, and Gosset et al., 1994b) gives the following results: the deformations appearing on the absorption components of the He I P Cygni profiles are well correlated in both the triplet and singlet series, as well as with the ones appearing in the N III absorptions (at least in N III  $\lambda 4097$  and N III  $\lambda 4103$ ). A closer inspection of these deformations relative to the overall mean spectrum indicates relative stability within the night (we will come back to this point in the next section) but a well-marked variability on a longer time-scale. This is illustrated in Fig. 6, where the three nightly mean profiles (of 1994) of the He I  $\lambda 4471$  line are plotted. The variation on the two consecutive nights is undoubtedly present, although weak, whereas the difference is conspicuous three weeks later.

These variations can be quantified through the mean of the radial velocities (hereafter RVs) of the four strongest He I absorptions, i.e.  $\lambda 3965$ ,  $\lambda 4026$ ,  $\lambda 4471$  and  $\lambda 4713$ . After heliocentric correction, the results are respectively  $-480 \text{ km s}^{-1}$ ,  $-487 \text{ km s}^{-1}$  and  $-424 \text{ km s}^{-1}$  for April 28/29, April 29/30 and May 21/22, 1994. By comparison, the Ca II interstellar absorption lines are stable within  $3 \text{ km s}^{-1}$  (one standard deviation) over the nightly mean spectra and within  $9.4 \text{ km s}^{-1}$  for the individual spectra, which means that the observed variations are

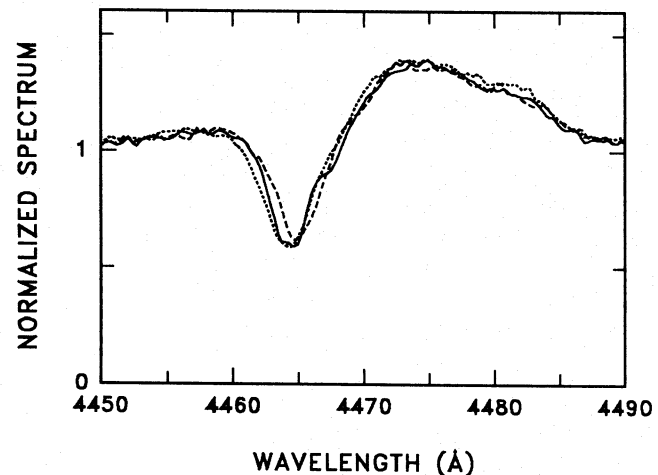


Fig. 6. Plot of the nightly mean of the He I  $\lambda 4471$  line profile for the 1994 nights of April 28/29 (continuous line), April 29/30 (dotted line) and May 21/22 (dashed line)

well above the measurement uncertainties. As mentioned earlier, the 1986 spectra are much noisier than the 1994 nightly means. Nevertheless, they are useful in the sense that they indicate that a variation of the absorption features by several tens of  $\text{km s}^{-1}$  can take place within two days.

For the emission lines, the situation is less clear. Surprisingly, no variation is detected for the N IV  $\lambda 4058$  line, which means that any possible variation in its intensity is buried in the noise. We measured the position of that line by fitting gaussian or empirical profiles. The derived mean position is not serviceable (because it is dependent on the adopted profile) but the related dispersion certainly is. A value  $\sigma = 0.34 \text{ \AA} \equiv 25 \text{ km s}^{-1}$  resulted from our measurements. This value is larger than the  $\sigma$  measured for the Ca II  $\lambda 3934$  line, but the difference in nature and width between the two lines can account for this. The one  $\sigma$  value presented here is to be considered as a statistical  $1\sigma$  upper limit on the variability in position of N IV  $\lambda 4058$ . The radial velocities of He II  $\lambda 4686$  have been measured on all the individual spectra. Although variations are present, particularly on the summit and on the blue wing of this line, a search for periodicities among this time series turned out to give no decisive result. Phase diagrams corresponding to the three photometric periods (see Sect. 3) have also been plotted. Only the period corresponding to  $1 + \nu_2$  is perhaps marginally seen in the variations of the positions of He II  $\lambda 4686$ .

#### 4.3. The short-term spectroscopic variability of WR 66

In order to study the short-term variability, we again constructed mean-normalized spectra but using now the nightly mean corresponding to the night under study, instead of the global mean. In such a context, we restrict ourselves to time-scales shorter than a day, and, indeed, most (but not all) of the variability observed in the absorption components of the P Cygni profiles disap-

pears. The noise is evidently larger than for the global mean and only two regions of the spectrum clearly vary within one night. These regions correspond to the top of the emission lines of He II  $\lambda 4686$  and N III  $\lambda\lambda 4634$ –4641. However, we should be cautious in our conclusions, because we are working with spectra initially normalized to the continuum and a pure variation of the continuum by itself could induce a similar phenomenon i.e. a detectable variation only at the top of the strongest lines. Therefore, when we report variations at the top of the strongest emission lines, they must be considered relative to the continuum level. One should be aware that the photometric variations represent one or two percent, which, translated to our spectroscopic data, very roughly corresponds to the level of the noise on one pixel of an individual spectrum. The top of the He II  $\lambda 4686$  emission line is variable and a cross-correlation of the pattern of deformation teaches us that the peak corresponding to N III  $\lambda 4641$  exhibits similar deformations. The case of the other peak (N III  $\lambda 4634$ ) is alike although a little more complex, probably because of interferences between different lines. A search for periodicities in these variations turned out to be inconclusive, but our sample is noisy and too limited for performing fully valid period searches, in most of the frequency domain. Consequently, this lack of a clear result should not be considered as definitive and a few points are worth being mentioned. As far as the emissions are concerned, the intensity of the deviations presented by He II  $\lambda 4686$  is not constant and actually seems to vary on a time-scale compatible with the photometric period reported in Sect. 3. By contrast, N IV  $\lambda 4058$ , which has been found to be strongly variable in the WN 6 star WR 134 (Vreux et al., 1992), is remarkably stable in WR 66. We show in Fig. 7 the raw plot of the relative intensities of the variations exhibited by the strongest lines as a function of time. By relative intensity, we mean the intensity on the global mean-normalized spectra integrated on a 4 Å wavelength domain centered on the line. Clearly, typical time-scales around a few hours characterize the observed variations (see Fig. 7). The recurrence of the signal is not precise enough, however, to reveal any periodicity. More numerous data and a better S/N ratio are necessary to allow any serious search for periodicities.

## 5. Discussion and conclusion

A high-frequency phenomenon has been detected in our photometric Strömgren *b*-band observations of WR 66 conducted in April 1989 and in June 1989, thus confirming in broad terms the results of Antokhin et al. (1995). The associated short period ( $\nu \sim 5.82 \text{ d}^{-1}$ ,  $P \sim 4\text{h}7\text{min} \sim 0.172 \text{ d}$ ) we derive is different from the value suggested by Antokhin et al. (1995), but this is just a matter of choice among a family of aliases. Therefore, both reported periods are quite compatible and can be considered up to now as identical. This agreement is important since, very often in the past, very short periodicities announced by one group have not been confirmed later on (see for example the case of WR 40). Here, instead, the same short period has been detected during two observing runs taking place four years apart (1989 for our observations, 1993 for the ones of Antokhin et al., 1995), with

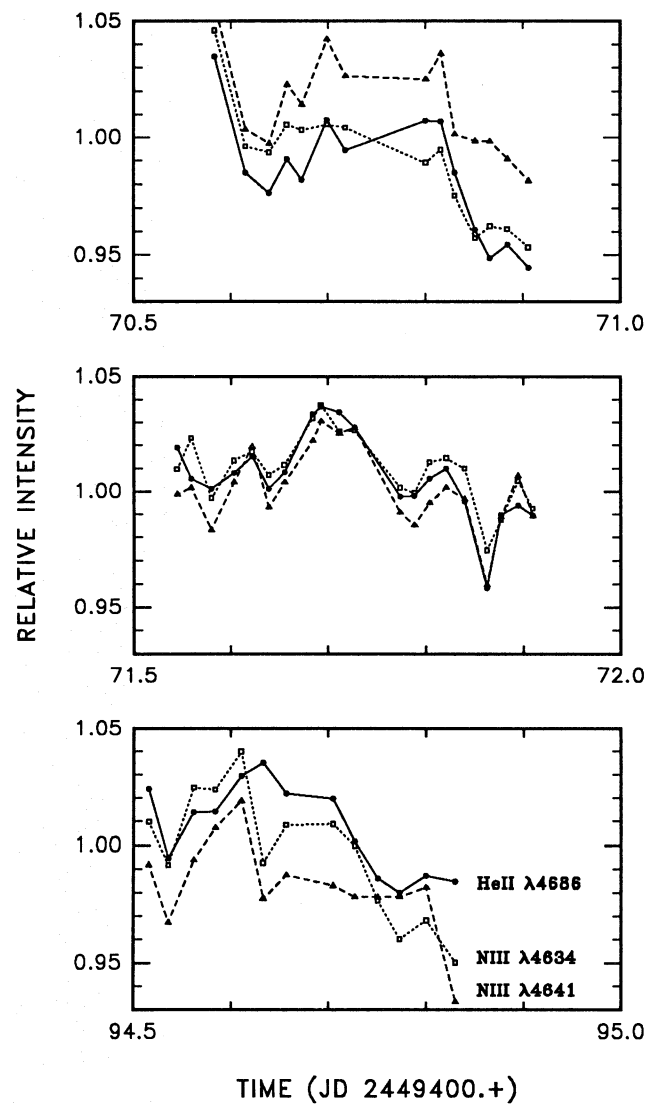


**Fig. 7.** Plot as a function of time of the relative intensity as integrated near the top of the lines of He II  $\lambda 4686$  (filled dots, continuous lines) and of N III  $\lambda 4641$  (triangles, dashed lines) and  $\lambda 4634$  (squares, dotted lines). The lines are given as a guide for the eyes. The basic time interval is 2.4 hours

totally different instruments and independent observing strategies. Of course, we have no proof of the uniqueness or of the stability of this frequency during the four years. Nevertheless, even if it is not permanently visible, the recurrence of such a frequency seems to indicate that it has a physical meaning and that we are not dealing with a particular realization of a stochastic process. In addition, if the intensity of the phenomenon is stable, the lower amplitude of the variations we observe through our *b* filter, when compared to the one observed by Antokhin et al. (1995) in the *V* band, suggests that most of the variation takes place in the continuum (as opposed to the lines) as is the case in other WR stars.

The spectroscopic observations, although noisy, give some interesting complementary information. The absorption compo-

nents of the P Cygni profiles point towards a non-steady mass loss along the column towards the star. At times, the amount of locally ejected material is increased, and this material is pushed away. But the signature is different from what is observed in the UV with the NAC (Narrow Absorption Component) in the sense that, in the present case, the signature is not particularly narrow since the whole absorption profile is modified and shifted. Neither the drift speed nor the periodicity or recurrence time-scale of these extra ejections is presently known. Nevertheless, if the photometric high frequency  $\nu_1$  is excluded, lower ones, like  $\nu_2$ , are quite possible. More spectroscopic observations of better quality are definitely needed.

Another interesting piece of information is given by the profile of N IV  $\lambda 4058$ , which is unexpectedly broad. This indicates that, in the wind of WR 66, a high degree of ionization is apparently maintained at a much higher distance from the star than in a typical late WN star.

In order to interpret these observations, the three following, usual, mechanisms have to be considered: radial pulsation, non-radial pulsation and binarity. Indeed, the period of about four hours is by far too short to be easily associated with the rotation of a massive star, as noticed by Antokhin et al. (1995). Present theoretical predictions about radial pulsations of WR stars favour periods in the range 15min to 60min (Maeder, 1985; Cox & Cahn, 1988; Maeder & Schaller, 1991). Lack or paucity of hydrogen in the external layers of the star is a necessary condition to avoid excessive radiative damping in the envelope. According to Maeder (1985), the unstable regime begins around H/He = 0.3, a condition satisfied by WR 66 (H/He = 0.2; Hamann, 1995; Hamann et al., 1995). However, the discrepancy on the period is as large as a factor of four, which is quite huge. The present WR models used to study instabilities do not take into account a series of characteristics such as, for example, the presence of an optically thick wind. These effects certainly have a great influence on the stability analyses; the future will teach us whether this is also true for the predicted frequencies. This is probably the case but not by such a large factor. Another explanation is that current evolutionary models could be poorly representative of WR stars and of their true extent. Clearly, more theoretical work is necessary before definitely ruling out the radial pulsation hypothesis.

By contrast, the observed period is within the range of those predicted for non-radial pulsations in some phases of WN evolution (Noels & Scuflaire, 1986). These phases correspond to the presence of a H-burning shell and are relatively short: one does therefore not expect to find many cases. The observed amount of hydrogen at the surface of WR 66 is compatible with the existence of such a shell. In addition, the mechanism described by Noels & Scuflaire (1986) easily explains the selective excitation of only one mode. The problem is that the nonadiabatic cases computed by Cox & Cahn (1988) do not support the conclusions of Noels and Scuflaire (1986) relative to the existence of unstable g-type non-radial modes in WN-like star models. Again, further theoretical works are needed. Indeed, all the previous considerations on pulsations are based on the classical idea that WR stars are related to stars evolved well off the main sequence.

Recently, Langer et al. (1994) suggested that the observed H-rich WNL stars could apparently be theoretically explained by core H-burning stars losing mass at a large rate due to newly identified vibrational instabilities. The H content of WR 66 is most probably too low to fit within this first theoretical WNL stage of evolution. Nevertheless, we will retain that, besides the classical modes, several authors identified in hot star models what they name strange modes. Recently, Glatzel et al. (1993) treated the case of WR stars and found, for the treated range of masses, periods still shorter than those associated with the fundamental radial mode.

Another alternative hypothesis is the binary model. The most common model consists of a WR star with a compact (degenerate) companion orbiting very close to it: for a wide range of plausible (and even implausible) values for the masses of both objects, the observed period implies, through Kepler's third law, a value of a few solar radii for the semi-major axis of the orbit, i.e. well within the wind of the WN 8 star (indeed, among all the WNL stars studied by Hamann et al. 1995, only three WN 6 stars have an estimated hydrostatic stellar core radius  $R_*$  lower than the derived upper limit on the semi-major axis). Under such a hypothesis, one would expect enhanced X-ray emission, which is not observed (Pollock et al., 1995; Norci & Meurs, 1994). Some scenarios have been considered to explain a lack of X-ray emission in binary WR+compact systems (Cherepashchuk & Moffat, 1994) and, consequently, the lack of such emission is not sufficient an argument to reject the binary hypothesis. Nevertheless, another observation weakens this scenario: the apparent lack (within the errors) of variability of N IV  $\lambda 4058$ . Due to the ionization degree involved and to some other characteristics of the transition, this line is produced rather deeply in the wind of a "standard" WN and thus should be sensitive to the presence of a compact companion being on such a deep orbit. The reported anomaly in the shape of this line, if not due to an orientation effect, could be the only visible signature of the binarity. However, we do not think that the solution of a compact object orbiting deeply in the wind, well below the whole N IV  $\lambda 4058$  emission formation region, is realistic: so deeply in the wind, the dynamical friction would severely reduce the lifetime of such an orbit. A counter-argument could reside in the existence of Cygnus X-3 (see e.g. Cherepashchuk & Moffat, 1994) which however is a strong X-ray emitter. The combination of the two arguments (lack of X-ray emission and lack of strong N IV variability) leads us to consider the binary mechanism as less promising than the other ones. More accurate observations of N IV  $\lambda 4058$  will probably be determinant; this line is particularly crucial, since it is suspected to be sensitive to the X-ray environment (Baum et al., 1992).

Another most interesting question is the study of the temporal behaviour of the variations of the mass ejection, as shown by the absorption lines. They could be periodic and linked in some way to the high frequency detected in the photometric data. If so, WR 66 could be a kind of Rosetta stone leading to the identification of the long-suspected extra-mechanism (in addition to radiation pressure) possibly implicated in the mass loss of WR stars and linking the latter to some kind of pulsation. The neces-

sity of such an extra-mechanism remains however unclear. We hope this paper will stimulate more observations of this interesting object in observatories where access to adequate telescopes is possible for this kind of research.

**Acknowledgements.** The authors are greatly indebted to L. Norci and E.J.A. Meurs for having examined ROSAT observations at their request and to I. Antokhin for having made results available in advance of publication. The authors would like to express their heartiest thanks to J. Breysacher (ESO) who allocated to them the 1.5m telescope when an unexpected opportunity took place in the original schedule of the instrument. Their thanks also go to P. Morris for discussions as well as to J.-P. Swings and F. Mélen who significantly improved a first version of the manuscript. The authors are also greatly indebted to the Fonds National de la Recherche Scientifique (Belgium) for multiple supports. This research is also supported in part by contracts ARC 90/94-140 and ARC 94/99-178 “Action de recherche concertée de la Communauté Française” (Belgium) and by contract SC005 of the belgian programme “Service Centers and Research Networks” initiated by the Belgian State, Prime Minister’s Office, Science Policy Programming under SSTC. Partial support through the PRODEX XMM-OM Project is also gratefully acknowledged. Part of the computations have been performed at the SEGI (Liège University). The SIMBAD database has been consulted for the bibliography.

## References

Antokhin, I., Bertrand, J.-F., Lamontagne, R., Moffat, A.F.J., Matthews, J. 1995, AJ, 109, 817

Baum, E., Hamann, W.-R., Koesterke, L., Wesselowsky, U. 1992, A&A, 266, 402

Cassinelli, J.P., Ignace, R., Bjorkman, J.E. 1995, in *Wolf-Rayet Stars: Binaries, Colliding Winds, Evolution*, proceedings of IAU Symposium No. 163, eds. K.A. van der Hucht & P.M. Williams, Dordrecht: Kluwer Acad. Publ., 191

Cherepashchuk, A.M., Moffat, A.F.J. 1994, ApJ, 424, L53

Conti, P.S., Massey, P., Vreux, J.-M. 1990, ApJ, 354, 359

Cox, A.N., Cahn, J.H. 1988, ApJ, 326, 804

Deeming, T.J. 1975, Ap&SS, 36, 137

Dennefeld, M., Guttin Lombard, B., Le Luyer, M., Rossignol, P. 1979, ESO Technical Note, IDG 120-79

ESO 1985, The Messenger, 41, 27

Glatzel, W., Kiriakidis, M., Fricke, K.J. 1993, MNRAS, 262, L7

Gosset, E., Rauw, G., Manfroid, J., Vreux, J.-M., Sterken, C. 1994a, in *The Impact of Long-term Monitoring on Variable Star Research*, proceedings of a NATO Advanced Research Workshop, eds. C. Sterken and M. de Groot, NATO ASI Series C, 436, 101

Gosset, E., Vreux, J.-M., Andrillat, Y. 1994b, in *Instability and Variability of Hot-Star Winds*, eds. A.F.J. Moffat, S.P. Owocki, A.W. Fullerton & N. St-Louis, Dordrecht: Kluwer Acad. Publ., Ap&SS, 221, 181

Gosset, E., Vreux, J.-M., Manfroid, J., Remy, M., Sterken, C. 1990, A&AS, 84, 377

Hamann, W.-R. 1995, in *Wolf-Rayet Stars: Binaries, Colliding Winds, Evolution*, proceedings of IAU Symposium No. 163, eds. K.A. van der Hucht & P.M. Williams, Dordrecht: Kluwer Acad. Publ., 105

Hamann, W.-R., Koesterke, L., Wesselowsky, U. 1993, A&A, 274, 397

Hamann, W.-R., Koesterke, L., Wesselowsky, U. 1995, A&A, in press

Horne, J.H., Baliunas, S.L. 1986, ApJ, 302, 757

van der Hucht, K.A., Conti, P.S., Lundström, I., Stenholm, B. 1981, Space Sci. Rev., 28, 227

Lamontagne, R., Moffat, A.F.J. 1987, AJ, 94, 1008

Langer, N., Hamann, W.-R., Lennon, M., et al. 1994, A&A, 290, 819

Loret, M.-C., Georgelin, Y.P., Georgelin, Y.M. 1987, A&A, 180, 65

Lundström, I., Stenholm, B. 1984, A&AS, 58, 163

Maeder, A. 1985, A&A, 147, 300

Maeder, A., Schaller, G. 1991, in *Wolf-Rayet Stars and Interrelations with Other Massive Stars in Galaxies*, proceedings of IAU Symposium No. 143, eds. K.A. van der Hucht & B. Hidayat, Dordrecht: Kluwer Acad. Publ., 167

Marchenko, S.V., Antokhin, I.I., Bertrand, J.-F. et al. 1994, AJ, 108, 678

Moffat, A.F.J. 1989, ApJ, 347, 373

Moffat, A.F.J., Robert, C. 1991, in *Wolf-Rayet Stars and Interrelations with Other Massive Stars in Galaxies*, proceedings of IAU Symposium No. 143, eds. K.A. van der Hucht & B. Hidayat, Dordrecht: Kluwer Acad. Publ., 109

Noels, A., Scuflaire, R. 1986, A&A, 161, 125

Norci, L., Meurs, E.J.A. 1994, private communication

Pollock, A.M.T., Haberl, F., Corcoran, M.F. 1995, in *Wolf-Rayet Stars: Binaries, Colliding Winds, Evolution*, proceedings of IAU Symposium No. 163, eds. K.A. van der Hucht & P.M. Williams, Dordrecht: Kluwer Acad. Publ., 512

Renson, P. 1978, A&A, 63, 125

Scargle, J.D. 1982, ApJ, 263, 835

Schmutz, W., Vacca, W.D. 1991, A&AS, 89, 259

Schwarz, H.E., Melnick, J. 1993, The ESO Users Manual, ed. European Southern Observatory, Garching bei München

Schwarzenberg-Czerny, A. 1989, MNRAS, 241, 153

Sterken, C., Manfroid, J. 1992, Astronomical Photometry: A Guide, Dordrecht: Kluwer Acad. Publ.

Vreux, J.-M., Dennefeld, M., Andrillat, Y. 1983, A&AS, 54, 437

Vreux, J.-M., Gosset, E., Bohannan, B., Conti, P.S. 1992, A&A, 256, 148

Westerlund, B.E. 1966, ApJ, 145, 724